Check for updates

NANO · MICRO small
www.small-journal.com

Extraordinary Acceleration of an Electrophilic Reaction Driven by the Polar Surface of 2D Aluminosilicate Nanosheets

*Nagy L. Torad, Yuta Tsuji, Azhar Alowasheeir, Masako Momotake, Kazuki Okazawa, Kazunari Yoshizawa, Michio Matsumoto, Masafumi Yamato, Yusuke Yamauchi, and Miharu Eguchi**

To increase chemical reaction rates, general solutions include increasing the concentration/temperature and introducing catalysts. In this study, the rate constant of an electrophilic metal coordination reaction is accelerated 23-fold on the surface of layered aluminosilicate (LAS), where the reaction substrate (ligand molecule) induces dielectric polarization owing to the polar and anionic surface. According to the Arrhenius plot, the frequency factor (*A*) is increased by almost three orders of magnitude on the surface. This leads to the conclusion that the collision efficiency between the ligands and metal ions is enhanced on the surface due to the dielectric polarization. This is surprising because one side of the ligand is obscured by the surface, so the collision efficiency is expected to be decreased. This unique method to accelerate the chemical reaction is expected to expand the range of utilization of LASs, which are chemically inert, abundant, and environmentally friendly. The concept is also applicable to other metal oxides which have polar surfaces, which will be useful for various chemical reactions in the future.

1. Introduction

To increase chemical reaction rates, general solutions include increasing reactant concentrations to increase collisions, raising the temperature to overcome the activation energy of the reactants, and using catalysts to decrease the activation energy. In this study, a 23-fold-increased rate constant for electrophilic metal coordination reactions was observed not by the abovementioned general solutions but by a surface of layered aluminosilicate (LAS). This increase is remarkable because the LAS is known to be chemically inert (no catalytic function), and the collision frequency is expected to decrease owing to the surface.

This work was motivated by our previous findings as follows. In 2017, we reported that the redox potential of an electrochromic material (iron(II) terpyridine) in the presence of LAS was lower than that in the absence of LAS,[1] as determined by cyclic voltammetry. X-ray photoelectron spectroscopy (XPS) measurements revealed that the Fe 2p binding energy decreased after adsorption, indicating that the cationic moiety (metal center, Fe^{2+}) of the metal complex was electrostatically neutralized by the anionic surface. Because the complex was electrochromic, this electrostatic neutralization reduced the working voltage of the electrochromic device. These results experimentally confirmed the perturbation

N. L. Torad, A. Alowasheeir, M. Momotake, M. Matsumoto, Y. Yamauchi, M. Eguchi
International Center for Nanoarchitectonics (MANA)
National Institute for Materials Science
1-1 Namiki, Tsukuba, Ibaraki 305-0044, Japan
E-mail: EGUCHI.Miharu@nims.go.jp

N. L. Torad, Y. Yamauchi, M. Eguchi
JST-ERATO Yamauchi Materials Space-Tectonics Project
National Institute for Materials Science
1-1 Namiki, Tsukuba, Ibaraki 305-0044, Japan

N. L. Torad
Chemistry Department
Faculty of Science
Tanta University
Tanta 31527, Egypt

The ORCID identification number(s) for the author(s) of this article can be found under https://doi.org/10.1002/smll.202205857.

© 2023 The Authors. Small published by Wiley-VCH GmbH. This is an open access article under the terms of the Creative Commons Attribution License, which permits use, distribution and reproduction in any medium, provided the original work is properly cited.

DOI: 10.1002/smll.202205857

Y. Tsuji, K. Okazawa, K. Yoshizawa
Institute for Materials Chemistry and Engineering
Kyushu University
744 Motooka, Nishi-ku 819-0395, Fukuoka, Japan

Y. Tsuji
Faculty of Engineering Sciences
Kyushu University
6-1, Kasuga-koen, Kasuga 816-8580, Fukuoka, Japan

M. Yamato
Department of Applied Chemistry for Environment
Tokyo Metropolitan University
1-1 Minami-Osawa, Hachioji 192-0397, Tokyo, Japan

Y. Yamauchi
Australian Institute for Bioengineering and Nanotechnology (AIBN) and School of Chemical Engineering
The University of Queensland
Brisbane, Queensland 4072, Australia

of the intramolecular electron distribution by electrostatic adsorption. Although the causality is simple, the electron distribution change of molecules on the surfaces and the effects on chemical properties have not been sufficiently studied.

Previous findings suggest that some chemical reactions should also be accelerated by LASs. However, at the same time, the lower collision frequency between substrates and reactants, because parts of the molecules are obscured by the surface is expected to decelerate the reaction. In this work, we aim to determine how to exploit the advantage of the electron distribution change of molecules on surfaces despite their obscuring.

Thus, in this study, the metal coordination reaction of a cationic porphyrin such as trimethylammoniophenyl porphyrin (H_2TMAP) was investigated as an example of an electrophilic reaction in the presence and absence of an LAS (Equations (1) and (2)).

$$H_2TMAP + Zn^{2+} \rightarrow Zn^{2+}TMAP + 2H^+ \quad (1)$$

$$H_2TMAP - LAS + Zn^{2+} \rightarrow Zn^{2+}TMAP - LAS + 2H^+ \quad (2)$$

Zn^{2+} was selected as the metal ion because zinc porphyrins do not readily undergo demetallization. In addition, zinc porphyrins are among the few porphyrins that exhibit a relatively long-lived excited singlet state, as demonstrated by their use in artificial photosynthesis systems. Another benefit of utilizing LAS is the possibility of optical observations due to its transparency in the visible region. The metal coordination reaction of the porphyrin molecules at the metal-vacuum interface was observed by surface science techniques such as scanning tunneling microscopy.[2] In these experiments, the activation energy was estimated by counting molecules one by one. In our system, the reaction rates in each case were determined from time-dependent absorption spectra. Furthermore, the causes of the differences in the rates are discussed based on data from solid-state NMR, XPS, and theoretical calculations. We believe that this novel method to improve chemical reactivity is an important approach owing to its simplicity and convenience compared with organic synthesis techniques such as the introduction of substituents.

2. Results and Discussion

H_2TMAP (**Figure 1**) was selected for this study to observe its metalation reaction in the presence and absence of LAS, which electrostatically binds to the cationic sites of porphyrins. Although tetrakis(1-methylpyridinium-4-yl) porphyrin (H_2TMPyP), which belongs to the same class of porphyrins (phyllo-type with occupied meso-positions), has also been examined for its photochemical properties on surfaces, it was not the focus of this study because its Q-band undergoes broadening on the surface of LASs and the spectral changes upon metalation are not as clear as those obtained for H_2TMAP. The degree of broadening is attributed to the flexibility of molecules. Less co-planarization of H_2TMAP upon adsorption prevents the broadening due to its bulky meso-substituents.

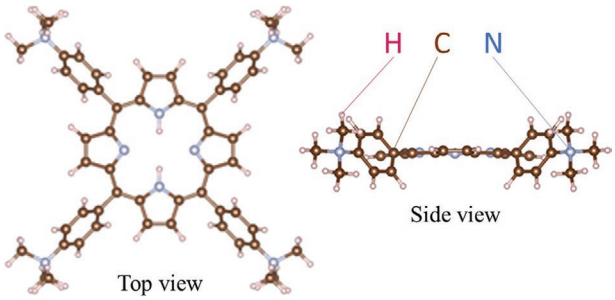

Figure 1. Optimized structure of H_2TMAP in a vacuum.

2.1. Structure of H_2TMAP in a Vacuum

The optimized structure of H_2TMAP in a vacuum calculated at the B3LYP/6-31G** level of theory using Gaussian 16 software is shown in Figure 1. The dihedral angle between the porphyrin ring and each trimethyl-anilinium group is estimated to be 63.73°. This angle is governed by the balance between the steric hindrance preventing rotation of the trimethyl-anilinium group and stabilization due to conjugation. The structure in water is considered to be identical. The dihedral angle is almost the same as that calculated for tetra-phenylporphyrin (H_2TPP) by the M05-2X density functional theory method.[3]

2.2. Electronic Distribution Transition upon Surface Adsorption; Absorption Spectra

Because the intercationic distance of H_2TMAP (1.31 nm) and the average interanionic distance of the LAS surface (1.20 nm) are similar, H_2TMAP can electrostatically bind to LAS in a monomeric fashion at up to 100% versus cation exchangeable capacity (CEC).[4] In other words, the cations and anions interact in a 1:1 ratio. The monomeric adsorption was confirmed by the unchanged absorption spectra at up to 100% versus CEC. The λ_{max} of the Soret band for H_2TMAP was 412 nm in water, and the peak redshifted by 12 nm upon binding to the surface.[4] The λ_{max} of the Q band (I) for H_2TMAP was 634 nm, and the peak redshifted by 12 nm upon adsorption. Adsorption onto graphene, metals, or aluminosilicates induced a decrease in the dihedral angle between the porphyrin ring and meso-substituents.[2,4–6] Some studies have evaluated the dependence of the shift widths of cationic porphyrins on the dihedral angle.[2,4] A smaller dihedral angle is accompanied by overall structural distortion and a higher energy, but the structure is stabilized by the entire system including the anionic surface because of the enthalpic stability afforded by the electrostatic attraction.[4] The smaller shift width for H_2TMAP than for H_2TMPyP (31 nm) was attributed to the smaller decrease in the dihedral angle due to the bulky trimethylanilinium groups. However, the change in the intramolecular electron distribution upon adsorption is not sufficiently well understood to control the chemical reactivity.

2.3. XPS

The N 1s XPS spectrum of H_2TMAP contained three peaks. The spectrum obtained with 500 cumulative scans is shown in

© 2023 The Authors. Small published by Wiley-VCH GmbH

16136829, 2023, 11, Downloaded from https://onlinelibrary.wiley.com/doi/10.1002/smll.202205857 by National Institute For, Wiley Online Library on [19/08/2024]. See the Terms and Conditions (https://onlinelibrary.wiley.com/terms-and-conditions) on Wiley Online Library for rules of use; OA articles are governed by the applicable Creative Commons License

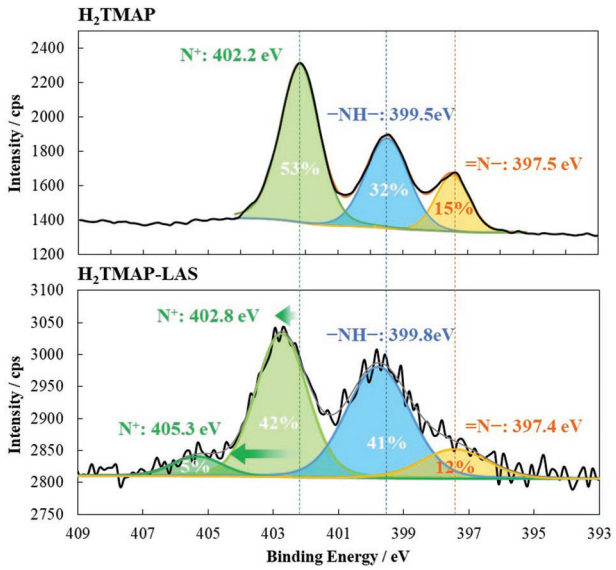

Figure 2. N 1s XPS spectra of H_2TMAP (top) and H_2TMAP-LAS (bottom). The black lines show the observed spectra. The yellow, blue, light green, and green lines show the obtained spectra after deconvolution. The thin gray line shows the superimposed spectrum. The percentages refer to the relative area for each deconvolved spectrum.

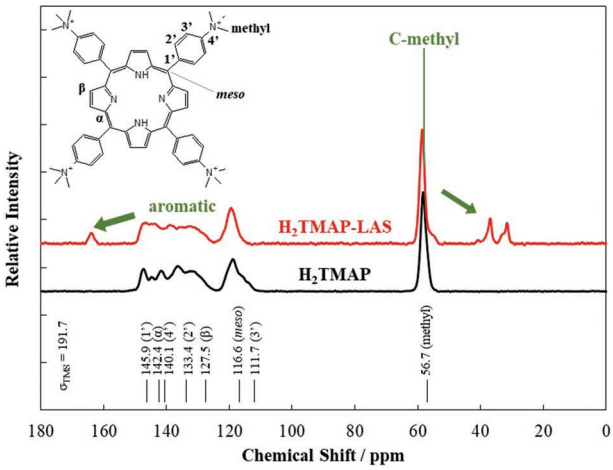

Figure 3. Solid-state ^{13}C NMR spectra of H_2TMAP with LAS (red line) and without LAS (black line).

Figure 2 (top). Deconvolution afforded three peaks centered at 402.2, 399.5, and 397.5 eV, which are assigned to N^+, −NH−, and =N−, respectively. The ratios of each species based on the chemical structure are 2:1:1 and their relative areas are 53, 32, and 15%. The rather small ratio of =N− is attributed to the damage by X-ray irradiation. The N^+ peak located at the highest energy as a result of the relatively low electron density because of the vicinity of the cation. Although the positive charge is conventionally written on the nitrogen atom, it should be noted that the cationic charge on the trimethyl-anilinium moiety of H_2TMAP (Figure 1) is localized on the methyl hydrogens owing to their lower electronegativity. The N 1s XPS spectrum for H_2TMAP-LAS is presented in Figure 2 (bottom). The total peak area was smaller (38%) than that for H_2TMAP because the signals are from several nanometers in depth where the density of H_2TMAP is diluted with LAS (1 nm thickness). Deconvolution of N 1s reveals the presence of four types of nitrogen states centered at 405.3, 402.8, 399.8, and 397.4 eV (relative areas: 5, 42, 41, and 12%). Judging from the peak positions and the relative areas, the two peaks at the highest binding energy are attributed to N^+, which is shifted to higher energy upon adsorption (Figure 2 (bottom)). A similar shift was reported for H_2TMPyP on LAS.[7] This shift is ascribed to the electrostatic neutralization due to the anionic surface, which is explained in detail below. The binding energy of N^+ is not identical on LAS because the distance between the cationic moiety of the porphyrin and the anionic charge on the surface cannot be always same since the anionic charges' distribution on the surface is random to some extent. The other two peaks do not exhibit a discernible shift, because only N^+ is the closest species to the cationic charges and thus its electron density is the most susceptible to adsorption. Increasing the number of scans to 2000 did not improve the signal-to-noise ratio, but the total area decreased. The deconvolved peak positions were consistent with those obtained after 500 scans. However, the relative area of the peak corresponding to =N− is decreased to 5%, which may indicate that this moiety is more sensitive to damage during X-ray irradiation.

2.4. Solid-State ^{13}C NMR

Solid-state ^{13}C NMR spectra were recorded for H_2TMAP (**Figure 3**, black line), LAS, and H_2TMAP-LAS (Figure 3, red line). Upon adsorption, drastic spectral changes were observed. In the case of H_2TMAP, the peak corresponding to the carbon atoms of the methyl groups (57.6 ppm) is observed in the typical region of carbon atoms in C−Cl bonds (electronegativity: 2.50 and 2.83). After adsorption, however, new peaks are emerged at 31.3 and 36.7 ppm, which lie in the typical region of carbon atoms in C−Br bonds (electronegativity: 2.50 and 2.74). This indicates that the electron density of these carbon atoms is magnified upon adsorption. Furthermore, the presence of multiple peaks for H_2TMAP-LAS suggests that the electron densities of the carbon atoms of the methyl groups are no longer equivalent after binding to the surface.

The peaks in the range of 110–150 ppm are assigned to the carbon atoms of the porphyrin and aniline rings, including the α, β, meso, 1′, 2′, 3′, and 4′ positions (atom labeling is depicted in the inset of Figure 3).[8] All seven peaks are not distinct for some reason, so each peak could not be assigned. The calculated chemical shifts and the assignments for H_2TMAP are superimposed at the bottom of Figure 3. Upon binding, some of these peaks are shifted to a lower field (163.5 ppm), which is the same region as carbon atoms bonded to oxygen. No peaks are observed for LAS itself as shown in Figure 3. As a reference, a solution-state ^{13}C NMR spectrum of H_2TMAP is presented in Figure S1, Supporting Information (left).

2.5. Solid-State ^{1}H NMR

The solid-state ^{1}H NMR spectrum of H_2TMAP without LAS contained three peaks centered at 8.23, 3.99, and 3.24 ppm as

© 2023 The Authors. Small published by Wiley-VCH GmbH

16136829, 2023, 11, Downloaded from https://onlinelibrary.wiley.com/doi/10.1002/smll.202205857 by National Institute For, Wiley Online Library on [19/08/2024]. See the Terms and Conditions (https://onlinelibrary.wiley.com/terms-and-conditions) on Wiley Online Library for rules of use; OA articles are governed by the applicable Creative Commons License

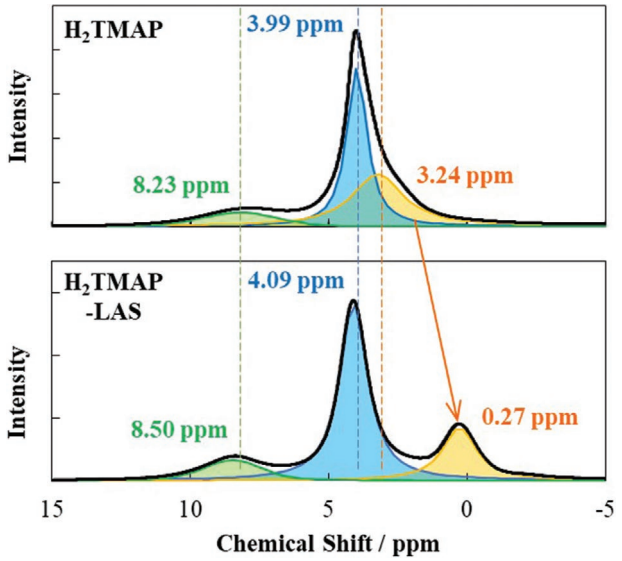

Figure 4. Solid-state ^{1}H NMR spectra of H_2TMAP (top) and H_2TMAP-LAS (bottom).

depicted in **Figure 4**. The peak at the lowest magnetic field is assigned to the aromatic ring protons, and the higher two peaks are assigned to the protons of the trimethyl groups. Therefore, although the methyl protons are equivalent and appeared as a quartet in the solution-state ^{1}H NMR spectrum (Figure S1, Supporting Information, right), they appeared not to be equivalent in the solid-state. For H_2TMAP with LAS, the peak at the highest field is shifted to 0.27 ppm (Figure 4). This observation is consistent with the results observed for C-methyl by solid-state ^{13}C NMR spectroscopy.

No peak corresponding to −NH− (known to occur between −2 and −3 ppm owing to the ring-current effect) is observed, although the reason for this remains unclear.

On the basis of the XPS and solid-state NMR results (summarized in Chart S1, Supporting Information), the proposed electron distribution changes at the $-N^{+}(CH_3)_3$ moieties of the trimethyl-anilinium groups due to adsorption are illustrated in **Figure 5**. In the absence of LAS, the cationic electrons are more uniformly delocalized over the hydrogen atoms owing to their relatively low electronegativity (Figure 5, left). In contrast, the peak shifts to a higher magnetic field in both ^{13}C and ^{1}H NMR spectroscopy upon binding with LAS, indicating that some of the carbon and hydrogen atoms of the methyl groups possess an increased electron density. This suggests the occurrence of dielectric polarization on the trimethyl-anilinium group due to the electric field originating from the anionic surface (Figure 5, right). This change in macroscopic properties is also consistent with the NMR results. The XPS analysis, on the other hand, reveals that the electron density is decreased at the nitrogen atoms of the trimethyl-anilinium group. This indicates that the localization of the electrons at the nitrogens due to their electronegativity is weaker, since the dielectric polarization enhances the electron density at some part of the methyl groups, as described above.

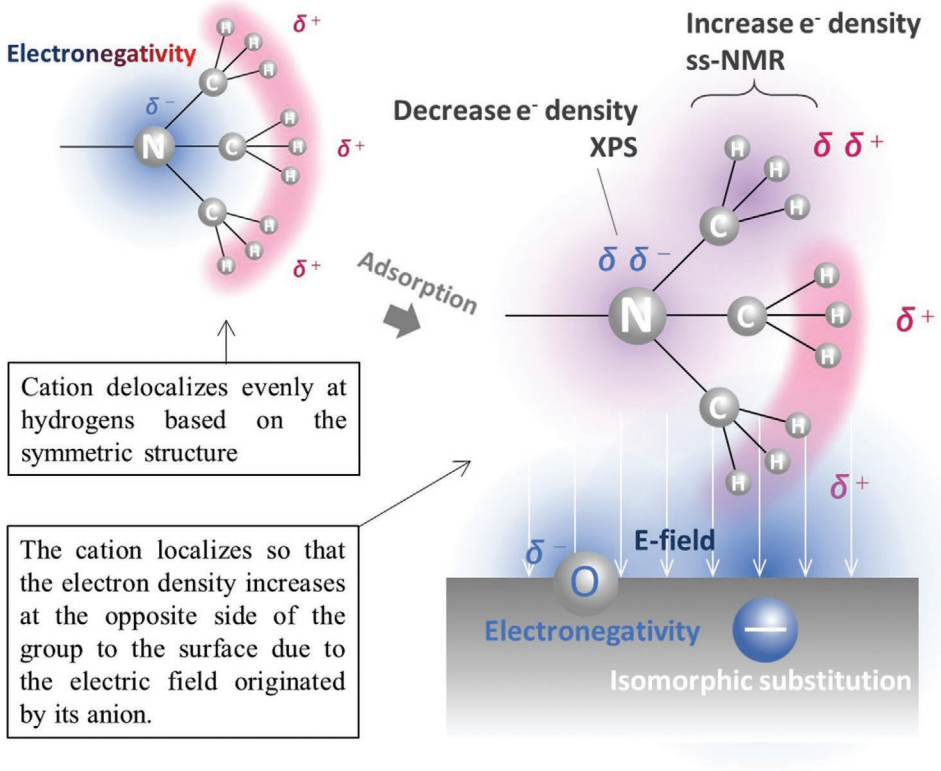

Figure 5. Proposed electron distribution changes at the trimethyl-anilinium groups due to the anionic surface based on the results of XPS and solid-state ^{1}H and ^{13}C NMR spectroscopy.

© 2023 The Authors. Small published by Wiley-VCH GmbH

16136829, 2023, 11, Downloaded from https://onlinelibrary.wiley.com/doi/10.1002/smll.202205857 by National Institute For, Wiley Online Library on [19/08/2024]. See the Terms and Conditions (https://onlinelibrary.wiley.com/terms-and-conditions) on Wiley Online Library for rules of use; OA articles are governed by the applicable Creative Commons License

With respect to the porphyrin ring, the electron densities at the −NH− and =N− moieties do not exhibit apparent shifts by XPS. In addition, although the ^{1}H and ^{13}C NMR peaks in the aromatic region are shifted to a lower magnetic field (less electron density), the identities of these peaks have not yet been determined.

2.6. Theoretical Calculations

Theoretical calculations were performed to obtain a more comprehensive understanding of the system. The LAS surface was modeled as a slab consisting of $Si_{112}O_{360}Al_8Mg_{60}H_{60}$ (600 atoms). The Al^{3+} ions were arranged such that the distances between them were 10.5 and 14.6 Å (Figure S2, Supporting Information, top). We considered two different adsorption patterns, taking into account the symmetry of the arrangement of atoms on the surface (Figure S2c,d, Supporting Information). It was found that the structure in which H_2TMAP is placed on the surface so that the distance between the carbon atoms of the methyl groups and the Al^{3+} ions is as small as possible is the most energetically favorable structure. Therefore, we adopted this as a model.

The average dihedral angle for H_2TMAP on LAS is found to be 61.3°, which is 2.4° smaller than that determined under vacuum. Compared with that when H_2TMPyP is adsorbed to the surface of LAS, the dihedral angle is smaller owing to the bulkier meso-substituents (trimethylanilinium groups).

Upon adsorption, an enhanced electron density (yellow area in **Figure 6**) is observed at both the outer face of the porphyrin (the side exposed to the solvent) and the oxygen on the LAS surface. In contrast, the electron density is found to decrease at the inner face of the porphyrin (light blue area in Figure 6).

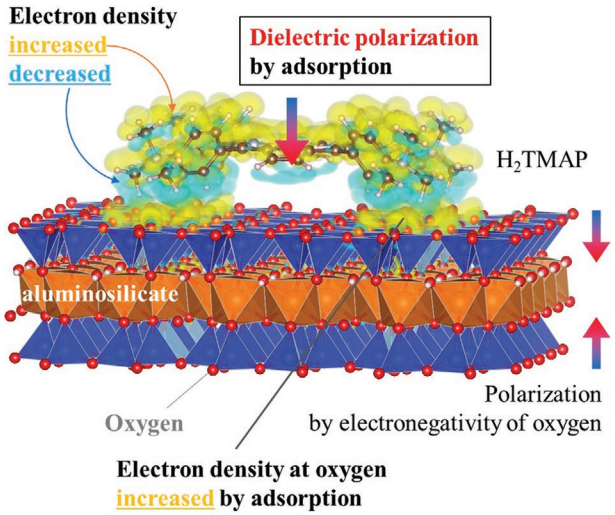

Figure 6. Theoretically calculated structure of H_2TMAP-LAS (side view). The red spheres indicate oxygen atoms. An isosurface plot of the charge density difference upon adsorption of H_2TMAP on the surface with an isodensity value of 0.007 e Å^{-3} is overlaid on the structure. The yellow and light blue areas indicate regions where the electron density increased and decreased, respectively.

The negatively charged surface also induced polarization in the normal direction of the porphyrin ring plane of H_2TMAP due to the high electronegativity of oxygen and the isomorphic substitution between Si^{4+} and Al^{3+}. The top view of the structure (Figure S3, Supporting Information) shows that the electron density increased all over the outer face after adsorption. The effect of surface polarization on the adjacent cell was minimized by introducing a sufficiently thick vacuum layer of 30 Å. The electrostatic potential profile is confirmed to be flat in the vacuum region, suggesting that the effects of surface polarization do not extend to the neighboring cell (Figure S4).

The theoretically simulated electron distribution after adsorption is consistent with that expected for the trimethyl-anilinium moiety based on the XPS and NMR results (Figure 5), and the simulation results indicate that similar dielectric polarization occurrs over the entire molecule upon binding to the anionic surface.

2.7. Metalation Reaction at the Surface

To provide a specific example of a chemical reaction that is accelerated on a surface, metal coordination by the cationic porphyrin was examined in this study (Prior to metalation, the protonation of H_2TMAP and H_2TMPyP was studied in the presence and absence of LAS. The details are described in the Supporting Information and in Figure S5, Supporting Information). To investigate this reaction, H_2TMAP and H_2TMAP-LAS were mixed with zinc(II) chloride in a specific molar ratio in water at room temperature (22 °C), and time-dependent absorption spectra were recorded (**Figure 7**). H_2TMAP exhibits a phyllo-type spectrum, in which the intensities of the Q-band peaks decrease in the order of IV > II > III > I (black lines in Figure 7). In general, the four peaks of the Q-band obtained for free-base porphyrins are observed as two peaks (α and β, where α occurs at a shorter wavelength) upon metal coordination.[9] At a 1:1 molar ratio, the difference in the reaction rates for metal coordination at 327 K in the absence and presence of LAS was not clear because of aggregate formation by LAS inclusion due to the longer reaction time hindered analysis such as deconvolution. To decrease the reaction time, the H_2TMAP:Zn^{2+} molar ratio was increased to 1:5, 1:10, 1:20, 1:30, and 0.5:20 (1:40). At these ratios, the reaction rate in the

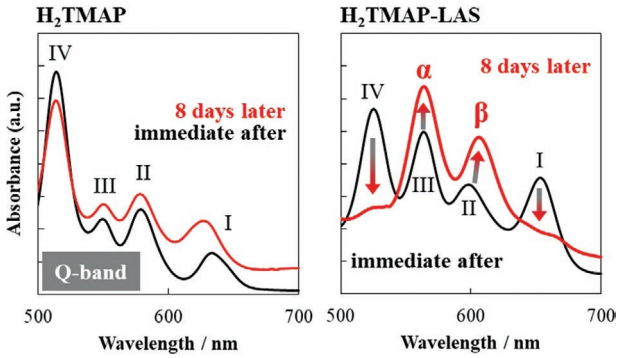

Figure 7. Q-band spectra for H_2TMAP immediately after mixing with $ZnCl_2$ (black lines) and after 8 days (red lines) in the absence (left) and presence (right) of LAS.

© 2023 The Authors. Small published by Wiley-VCH GmbH

16136829, 2023, 11, Downloaded from https://onlinelibrary.wiley.com/doi/10.1002/smll.202205857 by National Institute For, Wiley Online Library on [19/08/2024]. See the Terms and Conditions (https://onlinelibrary.wiley.com/terms-and-conditions) on Wiley Online Library for rules of use; OA articles are governed by the applicable Creative Commons License

presence of LAS was faster than that in the absence of LAS. The time-dependent changes in the spectral shapes of the Q-band obtained for H_2TMAP and H_2TMAP-LAS after mixing with zinc(II) chloride are presented in Figure 7. For stable observation, the molar ratio was fixed at 1:20. After 8 days, although the system without LAS remained unchanged (Figure 7, left), the system containing LAS showed two larger peaks (red line in Figure 7, right). A larger absorbance for the α peak than the β peak indicates the formation of a stable square-planar complex between the metal and the porphyrin.[9] This indicates that the electron densities of H_2TMAP and H_2TMAP-LAS are significantly different and that binding to LAS is advantageous for the metal coordination reaction.

2.8. Determination of the Frequency Factor and Activation Energy

The chemical reactions occurring in the absence and presence of LAS can be expressed in Equations (1) and (2).

The orders of the reaction (α, β) in Equation (3) were determined to be 1 and 2, respectively, based on the time-dependent spectra obtained at H_2TMAP:Zn^{2+} ratios of 1:5, 1:10, 1:20, 1:30, and 1:40 (at 327 K) in the presence and absence of LAS. The order of the reaction for metal coordination by porphyrin molecules depends on the combination of the metal ions, porphyrin structures, and their concentrations.[10] In the case of H_2TMAP and Zn^{2+}, the coordination reaction is expected to proceed via a multistep process including an intermediate.

The ratios at each time point were estimated by reproducing the spectrum based on those at the beginning and end of the experiment. The details of this calculation are described in the Supporting Information (Table S1, Supporting Information).

$$v = k[\mathrm{H_2TMAP}]^{\alpha}\left[\mathrm{Zn^{2+}}\right]^{\beta} \quad (3)$$

where $\alpha = 1$ and $\beta = 2$.

Then, the rate constants (k) at a ratio of 1:20 were calculated to be 8.74×10^4 and 2.00×10^6 L^2 mol^{-2} min^{-1} in the absence and presence of LAS, respectively. Thus, the rate constant increased 23-fold on the LAS surface. The details of this calculation are provided in the Supporting Information. Although this result was anticipated from the results of XPS, solid-state NMR spectroscopy, and protonation reaction experiments (Supporting Information), such an increase was surprising because the collision frequency of the metal coordination reaction is supposed to decrease owing to the LAS surface.

Thus, the rate constants were determined at three additional temperatures (301, 309, and 317 K) to generate an Arrhenius plot and estimate the frequency factor (A) and activation energy (E_a) based on the following equation (**Figure 8**, Table S1, Supporting Information).

$$k = \mathrm{Aexp}\left(-\mathrm{E_a} / \mathrm{RT}\right) \quad (4)$$

where R is the gas constant (J K^{-1} mol^{-1}) and T is the temperature (K).

The values of A and E_a were determined to be 1.55×10^{17} and 76.56 kJ mol^{-1} in the absence of LAS and 1.32×10^{20} and 86.59 kJ mol^{-1} in the presence of LAS, respectively.

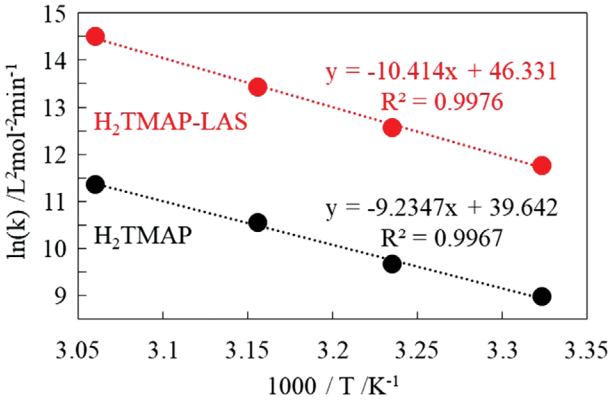

Figure 8. Arrhenius plot for the metal coordination reaction between Zn^{2+} and H_2TMAP (black circle) or H_2TMAP-LAS (red circle).

A comparison of the plotted data led to the following conclusions: 1) the reaction rate increased significantly when H_2TMAP was adsorbed on the LAS surface, 2) the values of activation energy remained similar regardless of the presence of LAS, and 3) the frequency factor increased significantly when H_2TMAP was adsorbed on the LAS surface. Therefore, the higher reaction rate was attributable to the higher frequency factor on the surface. This was an unexpected consequence because the frequency factor was expected to decrease owing to one side of the molecule being obscured by the surface, preventing the approach of the metal ions. However, this finding can be rationally explained from the observed and calculated structures, where the electron distribution is localized at the outer side of the molecules when they are bound to the surface. In this system based on LAS, more metal ions are electrostatically attracted to the outer surface of the molecules, such that the reaction rate increases despite the obstruction of the other side of the molecule. This is a remarkable example demonstrating that even chemically inert materials such as LASs have the potential to accelerate chemical reactions.

On the basis of a previous report suggesting that a smaller metal-nitrogen bond distance leads to a more stable metal-coordinated structure,[11] Cu^{2+}, which has a shorter metal-nitrogen bond (1.98 Å) than Zn^{2+} (2.05 Å), was added to the LAS-based system instead of Zn^{2+} to observe the effect on the reaction rate at room temperature (H_2TMAP : Cu^{2+} was 1:5 because the rate was too fast to observe for 1:20). The metal-coordination reaction was confirmed to be faster, in accordance with previous experiments, which were performed in solution (Figure S6, Supporting Information). Furthermore, a change in the time-dependent absorption after adding H_2TMAP (16% versus CEC) solution to the Cu^{2+}-LAS dispersion was observed. On this surface, the H_2TMAP:Cu^{2+} ratio was 1:12.5, where the amount of Cu^{2+} was high enough to show the reaction acceleration in a system using the parent LAS. However, the spectral change, which indicates metal coordination, was not observed in this system. This result eliminates the possibility that the acceleration of the coordination reaction occurs due to the concentration of metal ions at the surfaces. Counter cations presumably distribute evenly on the surface according to the disposition of surface anions, so that the concentration

© 2023 The Authors. Small published by Wiley-VCH GmbH

16136829, 2023, 11, Downloaded from https://onlinelibrary.wiley.com/doi/10.1002/smll.202205857 by National Institute For, Wiley Online Library on [19/08/2024]. See the Terms and Conditions (https://onlinelibrary.wiley.com/terms-and-conditions) on Wiley Online Library for rules of use; OA articles are governed by the applicable Creative Commons License

of cations will not be high enough to show the reaction rate acceleration. At the same time, the desorption of two Cu^{2+} ions due to the adsorption of a H_2TMAP molecule (four-valent) may disturb the efficient interaction between them.

3. Conclusion

In this study, we determined how the rate constant of the electrophilic reaction was increased on the surface of the LAS even though the surface obscures the collision of reactants. We concluded that the localized electron at the outer side of molecules in the complex electrostatically accelerates the electrophilic reaction of metal ions, which results in the enhancement of the frequency factor at the surface. Although this type of LAS is chemically stable and has no catalytic function, its effect on the electron distribution was greater than we expected (23-fold compared with the solution system). At least when the molar ratio of Zn^{2+} is more than five relative to that of TMAP, the impact of increasing of the frequency factor exceeds the impact of surface obscuration.

Although the acceleration of the reaction by controlling activation energies has been widely studied using catalysis, controlling the frequency factors without increasing the concentration has not been well explored. Thus, this approach would be a new strategy to improve the reaction rates of chemical reactions such as organic synthesis. We anticipate the same effect for various inorganic anionic surfaces, including niobium or titanium salts, or even metal oxides with polar surfaces. For photochemical device fabrication, the reported method may be applicable in one-pot syntheses of organic–inorganic hybrid complexes such as artificial photosynthetic systems.

4. Experimental Section

LAS, a swellable 2:1 layered synthetic silicate with a tri-octahedral sheet ($[(Si_{7.20}Al_{0.80})(Mg_{5.97}Al_{0.03})O_{20}(OH)_4]^{-0.77}(Na_{0.77})^{+0.77}$), was provided by Kunimine Industries and was purified by repeated decantation from water and washing with ethanol. Surfaces were typically obtained by full exfoliation in water to prepare single layers of LASs. The thickness of each sheet was 1 nm, and the surface was flat at the atomic level. Exchangeable cationic ions, such as sodium ions, could be replaced by cationic substances. Cu^{2+}-LAS was prepared by dispersing LAS powder into a $CuCl_2$ solution, followed by repeated washing using centrifugation with distilled water. *p*-Toluenesulfonate salts of 5,10,15,20-tetrakis(4-trimethylammoniophenyl)porphyrin (H_2TMAP) and tetrakis(1-methylpyridinium-4-yl) porphyrin (H_2TMPyP) were obtained from Sigma Aldrich and Frontier Scientific, respectively, and the counterions were exchanged to Cl^- using an ion-exchange resin (H_2 denotes the free-base form). Distilled water was purchased from Fujifilm. Buffer solutions at various pH values were prepared by mixing sodium hydroxide, 1 M hydrochloric acid, and potassium hydrogen phthalate (all from Fujifilm) at the appropriate concentrations.

Porphyrin-LAS complexes were prepared by mixing a porphyrin solution and a LAS dispersion. These species combined through electrostatic attraction.[4,12,13] The loading level was 16% versus CEC for the absorptiometer samples and 100% versus CEC for the XPS and NMR samples. LASs were ideal materials for evaluating the structures and properties of adsorbed molecules because they were chemically inert and have a precisely determined shape.[7,14–18] In addition, the occupied area per anion of 1.25 nm^2 (average distance between anionic sites: 1.20 nm) on the surface was favorable for the adsorption of molecules because it was comparable to a typical molecular cross-section.[13a] A tetra-cationic porphyrin, H_2TMPyP, whose distance between adjacent cationic sites was 1.05 nm, was known to adsorb onto the surface in the same manner as the monomer with up to 100% of the CEC.[12,13a] This indicated that the cationic sites of the porphyrin and the anionic sites of the surface interacted in a 1:1 ratio. It should be noted that the adsorption equilibrium constant for this system was large, with all of the porphyrin molecules adsorbing immediately to the surface at loading levels of less than 100% versus CEC in water.[5] Furthermore, it was recently revealed that the N 1s XPS spectra of H_2TMPyP indicated an increase in the binding energy of the pyridinium N^+ atoms and a decrease in that of the internal =N− moieties at the surface of the LAS.[6] These changes in the electron distribution around nitrogen due to the anionic surface suggested that such surfaces may alter the reaction rates of substrates by inducing a particular electron distribution. Based on this suggestion, it was hypothesized that an electrophilic reaction such as a metal coordination reaction occurred at the internal =N− moieties of porphyrin molecules could be accelerated on the surface of LAS.

XPS analysis was performed on a Quantum-2000 system (ULVAC-PHI). Tablet samples with a diameter of 10 mm were prepared from LAS, H_2TMAP, and their hybrid complex using a tablet press. The excitation source was Al–Kα, and the X-ray tube voltage was 15 kV. The pass energy was 58.7 eV, and the step size was 0.125 eV. The cumulative number of scans was 500 or 2000 for N 1s and 50 for C 1s. The horizontal axis was corrected based on the peak position of C 1s at 284.5 eV.

Solid-state ^{13}C NMR spectroscopy was performed on a JEM-ECA400 system (JEOL) with a ^{13}C cross polarization-magic angle spinning-total suppression of spinning sideband, a frequency of 100.5253 MHz, a spectral width of 40.2 kHz, a pulse width of 3.34 µs, 2048 observation points, a cumulative waiting time of 5 s, and a sample rotation frequency of 6 kHz at room temperature. Powder samples of H_2TMAP, LAS, and their hybrid complex (100% loading versus CEC) were used. Solid-state ^{1}H NMR spectroscopy was conducted on an Ascend TM400 instrument (Bruker) with ^{1}H magic angle spinning, a frequency of 400.1709844 MHz, a spectral width of 100 kHz, a pulse width of 3.8 µs, 2048 observation points, a cumulative waiting time of 5 s, 16 scans, and a sample rotation frequency of 10, 12, or 15 kHz at room temperature. The samples were the same as those used for the solid-state ^{13}C NMR experiments. In both cases, the horizontal axis was corrected using an external standard (adamantane).

Solution-state ^{1}H NMR and ^{13}C NMR spectroscopy were performed on a JNM-ECX400 system (JEOL). H_2TMAP was dissolved in deuterium oxide. The chemical shift values were referenced to the solvent residual carbon signal as an internal standard (deuterium oxide for ^{1}H NMR and methanol for ^{13}C NMR).

Absorption spectra were recorded on a UV2600 spectrometer (Shimadzu). The samples were transferred to quartz cuvettes with an optical path length of 10 mm. A temperature controller (TCC-240A, Shimadzu) was attached to evaluate the temperature dependence.

The structure of H_2TMAP^{4+} in a vacuum was optimized using Gaussian 16[19] at the B3LYP-D3(BJ)/6-31G** level of theory.[20] The structure of H_2TMAP adsorbed on the LAS surface was determined by optimizing the structure of a periodic slab model using VASP version 5.4.4.[21] Details of the slab model construction are described in the Supporting Information (see Figure S2, Supporting Information). The PBE functional[22] with the D3(BJ) dispersion correction scheme was adopted. The electron-ion interactions were treated within the projector augmented wave scheme.[23] A plane-wave basis set cutoff of 400 eV, a self-consistent field tolerance of 1.0×10^{-5} eV, Brillouin zone sampling on a grid with a spacing of $2\pi \times 0.05$ Å^{-1}, and a 0.03 eV Å^{-1} threshold of atomic forces were used. The theoretically calculated structures presented throughout this paper were visualized using VESTA.[24]

Supporting Information

Supporting Information is available from the Wiley Online Library or from the author.

© 2023 The Authors. Small published by Wiley-VCH GmbH

16136829, 2023, 11, Downloaded from https://onlinelibrary.wiley.com/doi/10.1002/smll.202205857 by National Institute For, Wiley Online Library on [19/08/2024]. See the Terms and Conditions (https://onlinelibrary.wiley.com/terms-and-conditions) on Wiley Online Library for rules of use; OA articles are governed by the applicable Creative Commons License

Acknowledgements

The authors are grateful to Prof. Thomas E. Mallouk at the University of Pennsylvania for valuable comments. This work was supported by KAKENHI (19K05641) and JST-ERATO Yamauchi Materials Space-Tectonics Project (JPMJER2003). The computations in this work were primarily performed using the computer facilities at the Research Institute for Information Technology, Kyushu University. Y.T. is grateful for KAKENHI grants (numbers JP21K04996 and JP22H05146). This work was performed in part at the Queensland node of the Australian National Fabrication Facility, a company established under the National Collaborative Research Infrastructure Strategy to provide nano- and microfabrication facilities for Australia's researchers.

Open access publishing facilitated by The University of Queensland, as part of the Wiley - The University of Queensland agreement via the Council of Australian University Librarians. [Correction added after publication 15 March 2023: Eq. 1 and 2 were corrected.]

Conflict of Interest

The authors declare no conflict of interest.

Data Availability Statement

The data that support the findings of this study are available on request from the corresponding author. The data are not publicly available due to privacy or ethical restrictions.

Keywords

aluminosilicates, anionic surfaces, collision frequency, dielectric polarization, electrostatic interaction, inert surfaces, metal coordination reaction, porphyrin

Received: September 24, 2022
Revised: November 11, 2022
Published online: January 9, 2023

[1] M. Eguchi, M. Momotake, F. Inoue, T. Oshima, K. Maeda, M. Higuchi, *ACS Appl. Mater. Interfaces* **2017**, *9*, 35498.
[2] a) J. M. Gottfried, K. Flechtner, A. Kretschmann, T. Lukasczyk, H.-P. Steinrück, *J. Am. Chem. Soc.* **2006**, *128*, 5644; b) F. Buchner, V. Schwald, K. Comanici, H.-P. Steinrück, H. Marbach, *ChemPhysChem* **2007**, *8*, 241; c) W. Auwärter, A. Weber-Bargioni, S. Brink, A. Riemann, A. Schiffrin, M. Ruben, J. V. Barth, *ChemPhysChem* **2007**, *8*, 250; d) H. Marbach, *Acc. Chem. Res.* **2015**, *48*, 2649.
[3] V. A. Karachevtsev, S. G. Stepanian, M. V. Karachevtsev, L. Adamowicz, *Comput. Theor. Chem.* **2018**, *1133*, 1.
[4] Z. Chernia, D. Gill, *Langmuir* **1999**, *15*, 1625.
[5] S. Takagi, D. A. Tryk, H. Inoue, *J. Phys. Chem. B* **2002**, *106*, 5455.
[6] M. Eguchi, A. S. Nugraha, A. E. Rowan, J. Shapter, Y. Yamauchi, *Adv. Sci.* **2021**, *8*, 2100539.
[7] Y. Date, Y. Kagawa, R. Sasai, K. Kohno, E. Hino, T. Fujii, K. Aoki, K. Oda, *Clay Sci.* **2015**, *19*, 85.
[8] D. Mohajer, S. Zakavi, S. Rayati, M. Zahedi, N. Safari, H. R. Khavasib, S. U. Shahbazian, *New J. Chem.* **2004**, *28*, 1600.
[9] R. Giovannetti, in *Macro to Nano Spectroscopy* (Ed: J. Uddin), IntechOpen, London **2012**, pp. 87–108.
[10] S. Funahashi, Y. Yamaguchi, M. Tanaka, *Bull. Chem. Soc. Jpn.* **1984**, *57*, 204.
[11] E. B. Fleischer, *Acc. Chem. Res.* **1970**, *3*, 105.
[12] V. G. Kuykendall, J. K. Thomas, *Langmuir* **1990**, *6*, 1350.
[13] a) M. Eguchi, S. Takagi, H. Tachibana, H. Inoue, *J. Phys. Chem. Solids* **2004**, *65*, 403; b) M. Eguchi, T. Shimada, H. Inoue, S. Takagi, *J. Phys. Chem. C* **2016**, *120*, 7428; c) Y. Ishida, D. Masui, T. Shimada, H. Tachibana, H. Inoue, S. Takagi, *J. Phys. Chem. C* **2012**, *116*, 7879.
[14] a) J. Bujdák, *J. Photochem. Photobiol.* **2018**, *35*, 108; b) J. Bujdák, N. Iyi, R. Sasai, *J. Phys. Chem. B* **2004**, *108*, 4470.
[15] K. Bergmann, C. T. O'Konski, *J. Phys. Chem.* **1963**, *67*, 2169.
[16] J. Bujdák, N. Iyi, Y. Kaneko, R. Sasai, *Clay Miner.* **2003**, *38*, 561.
[17] F. L. Arbeloa, V. M. Martínez, *Chem. Mater.* **2006**, *18*, 1407.
[18] R. Sasai, H. Miyanaga, M. Morita, *Clay Sci.* **2013**, *17*, 35.
[19] M. J. Frisch, G. W. Trucks, H. B. Schlegel, G. E. Scuseria, M. A. Robb, J. R. Cheeseman, G. Scalmani, V. Barone, G. A. Petersson, H. Nakatsuji, X. Li, M. Caricato, A. V. Marenich, J. Bloino, B. G. Janesko, R. Gomperts, B. Mennucci, H. P. Hratchian, J. V. Ortiz, A. F. Izmaylov, J. L. Sonnenberg, D. Williams-Young, F. Ding, F. Lipparini, F. Egidi, J. Goings, B. Peng, A. Petrone, T. Henderson, D. Ranasinghe, et al. Gaussian, Inc., Wallingford CT **2016**.
[20] S. Grimme, S. Ehrlich, L. Goerigk, *J. Comput. Chem.* **2011**, *32*, 1456.
[21] a) G. Kresse, J. Hafner, *Phys. Rev. B: Condens. Matter Mater. Phys.* **1993**, *47*, 558; b) G. Kresse, J. Hafner, *Phys. Rev. B: Condens. Matter Mater. Phys.* **1994**, *49*, 14251; c) G. Kresse, J. Furthmüller, *Comput. Mater. Sci.* **1996**, *6*, 15; d) G. Kresse, J. Furthmüller, *Phys. Rev. B: Condens. Matter Mater. Phys.* **1996**, *54*, 11169.
[22] J. P. Perdew, K. Burke, M. Ernzerhof, *Phys. Rev. Lett.* **1996**, *77*, 3865.
[23] a) G. Kresse, D. Joubert, *Phys. Rev. B* **1999**, *59*, 1758; b) B. Adolph, J. Furthmüller, F. Beckstedt, *Phys. Rev. B* **2001**, *63*, 125108.
[24] K. Momma, F. Izumi, *J. Appl. Cryst.* **2011**, *44*, 1272.

© 2023 The Authors. Small published by Wiley-VCH GmbH

16136829, 2023, 11, Downloaded from https://onlinelibrary.wiley.com/doi/10.1002/smll.202205857 by National Institute For, Wiley Online Library on [19/08/2024]. See the Terms and Conditions (https://onlinelibrary.wiley.com/terms-and-conditions) on Wiley Online Library for rules of use; OA articles are governed by the applicable Creative Commons License